Accessible Method for the Development of Novel Sterol Analogues with Dipeptide-like Side Chains That Act as Neuroinflammation Inhibitors

Hongli Chen,[*,†,§] Chaojun Han,[‡,§] Jing Wu,[‡,§] Xiaoyu Liu,[†] Yuexiong Zhan,[†] Jiakang Chen,[†] Yanke Chen,[‡] Ruinan Gu,[‡] Li Zhang,[‡] Shuangshuang Chen,[‡] Jia Jia,[‡] Xuechu Zhen,[‡] Long Tai Zheng,[*,‡] and Biao Jiang[*,†]

[†]Shanghai Institute for Advanced Immunochemical Studies, ShanghaiTech University, Shanghai 201210, China
[‡]Jiangsu Key Laboratory of Translational Research and Therapy for Neuropsychiatric Diseases and College of Pharmaceutical Sciences, Soochow University, Suzhou, Jiangsu 215021, China

Ⓢ *Supporting Information*

ABSTRACT: A number of novel sterol derivatives with dipeptide-like side chains were synthesized using an Ugi four-component condensation method and assayed to test their anti-inflammatory effects in activated microglial cells. Compound **18b** ((3S,10R,13S)-N-((R)-1-(*tert*-butylamino)-1-oxo-3-phenylpropan-2-yl)-3-hydroxy-N,10,13-trimethyl-2,3,4,7,8,9,10,11,12,13,14,15-dodecahydro-1H-cyclopenta[a]-phenanthrene-17-carboxamide) was identified as the most potent anti-inflammatory agent in the series of compounds analyzed. Compound **18b** markedly inhibited the expression of proinflammatory factors, including inducible nitric oxide synthase, interleukin (IL)-6, IL-1β, tumor necrosis factor-α, and cyclooxygenase-2 in lipopolysaccharide-stimulated microglial cells. Further studies showed that compound **18b** significantly suppressed the transcriptional activity of AP-1 and NF-κB in activated microglial cells, which was likely mediated by the inhibition of the p38 MAPK and JNK signal transduction pathways. In addition, compound **18b** displayed neuroprotective effects in a microglial-conditioned medium/neuron coculture and an experimental focal ischemic mouse model.

KEYWORDS: Ugi four-component condensation, microglia, neuroinflammation, neuroprotection, focal ischemic mouse model
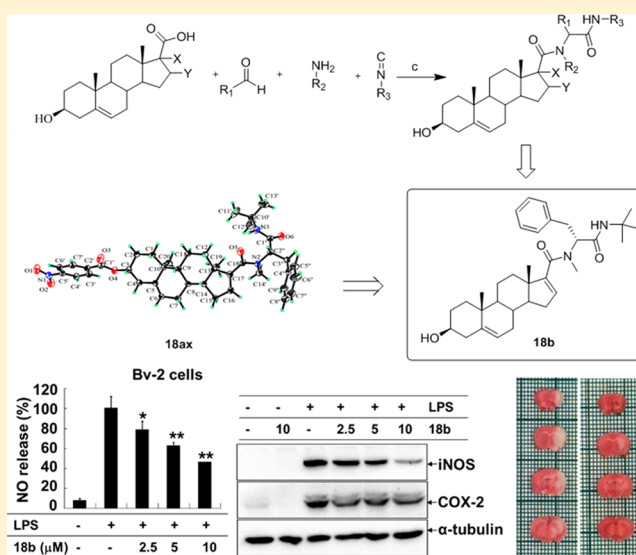
Sustained and excessive neuroinflammation is actively involved in the pathogenesis of many central nervous system (CNS) diseases, such as ischemic stroke, trauma, Parkinson's disease, multiple sclerosis, and Alzheimer's disease.[1−3] As the resident immune cells in the brain and spinal cord, microglia not only monitor the brain's environment and/or provide nutrition to maintain brain homeostasis but also play a critical role in the regulation of neuronal survival.[4] Once activated, microglia produce a variety of proinflammatory cytokines and free radicals, such as nitric oxide (NO), tumor necrosis factor-α (TNF-α), interleukin-1β (IL-1β), interleukin-6 (IL-6), and reactive oxygen species (ROS), that induce neuronal cell damage.[1] There is increasing evidence that the inhibition of microglia-mediated neuroinflammation is an important and direct strategy for treating neurodegenerative diseases.[5] Therefore, the development of new antineuroinflammatory agents that target microglial activation is an important strategy in the discovery of drugs for the treatment of neuroinflammatory disorders.

Biomedical research has demonstrated that some steroids, such as dehydroepiandrosterone (DHEA), progestogens, androgens, and estrogens, are involved in a variety of CNS functions, including the reduction of neuroinflammation.[6] Studies conducted so far suggest that steroids are an attractive source for the discovery of antineuroinflammatory agents. DHEA, which displays antineuroinflammatory activity via the inhibition of lipopolysaccharide (LPS)-induced NO production in BV-2 microglia[7] was employed as a positive control in our studies. We found that compound **1** (Figure 1) showed
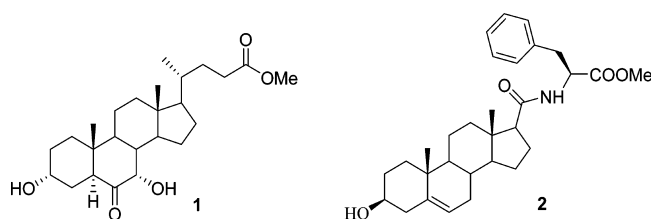
Figure 1. Structures of compounds **1** and **2**.

Table 1. Structures of Compounds 9a–18b

compd	X, Y	R$_1$	R$_2$	R$_3$
9a/9b	double bond	CH(CH$_3$)$_2$	CH$_3$	C(CH$_3$)$_3$
10a/10b	single bond	CH(CH$_3$)$_2$	CH$_3$	C(CH$_3$)$_3$
11a/11b	single bond	CH(CH$_3$)$_2$	CH$_2$Ph	C(CH$_3$)$_3$
12a/12b	single bond	CH$_2$Ph	CH$_3$	C(CH$_3$)$_3$
13a/13b	single bond	Ph	CH$_3$	C(CH$_3$)$_3$
14a/14b	X = H, Y = CH$_3$	CH(CH$_3$)$_2$	CH$_3$	C(CH$_3$)$_3$
15a/15b	double bond	cyclohexyl	CH$_3$	C(CH$_3$)$_3$
16a/16b	double bond	CH(CH$_3$)$_2$	CH$_3$	m-xylene
17a/17b	X = H, Y = CH$_3$	Ph	CH$_3$	C(CH$_3$)$_3$
18a/18b	double bond	CH$_2$Ph	CH$_3$	C(CH$_3$)$_3$

beneficial biological activities. This compound is a synthetic 5α-cholestan-6-one sterol analogue that inhibits the microglia-mediated inflammatory response by blocking the increase in the production of NO, IL-1β, and TNF-α and reducing infarction volume in a focal ischemic mouse model.[8] Recently, we have also reported that an androstene-sterol derivative, compound **2**, exhibited a higher antineuroinflammatory potency than compound **1**.[9] As part of our ongoing sterol neuroinflammation inhibitor discovery and development program, we are interested in the generation of sterol scaffolds with dipeptide-like side chains using a simple and fast procedure, Ugi four-component condensation (U-4CC), in which an aldehyde, an amine, a carboxylic acid, and an isocyanide react together to give α-aminoacyl amide derivatives.[10−13] U-4CC is one of the most well-known and efficient multicomponent reactions and is widely used in medicinal chemistry.

In this study, we have successfully applied U-4CC to produce a new family of sterol derivatives. The antineuroinflammatory capacities of these synthetic compounds and their underlying mechanisms were assessed in microglial cells. The result show that compound **18b** exhibited the most potent anti-inflammatory properties among this family. Compound **18b** also significantly inhibited the expression of proinflammatory genes and suppressed signal transduction molecules, such as p38 MAPK, JNK, and transcription factor AP-1. Furthermore, compound **18b** exhibited neuroprotective properties *in vitro* and *in vivo*.
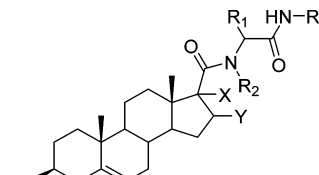
■ RESULTS AND DISCUSSION

Chemistry. Sterol analogues with dipeptide-like side chains were synthesized by means of the highly efficient and versatile U-4CC. The general synthetic route for the synthesis of target compounds **9a–18b** (Table 1) is outlined in Scheme 1. The steroidal 17-carboxylic acids (**4**, **7**, and **8**) were synthesized from pregnenolone (**3**) or 16-dehydropregnenolone (**5**) as described in the literature.[14] Treatment of the acid with an aldehyde, an amine, and an isocyanide led to the formation of the desired compounds in a 1:1 diastereomeric mixture with moderate to good yields (58−96%).

The structures of all synthesized compounds were identified by ^{1}H NMR, ^{13}C NMR, MS, HR-MS, and optical rotation. X-ray diffraction of the crystal obtained from the mixture of compounds **9a** and **9b** confirmed the structure of these products (Figure 2A). Although all of the pairs of stereoisomers could be separated by column chromatography or Pre-HPLC, the R,S configuration corresponding to each isomer could not be assigned unless the crystal of a single compound was obtained and subjected to X-ray analysis. The crystalline structure of compound **9a** was used to established the absolute configuration of S at the stereocenter (Figure 2B)

Pharmacology. NO is an important neuroinflammatory factor that is secreted by activated microglial cells and contributes to neuronal damage and apoptosis.[1] Thus, the

inhibitory effects of compounds **9a−18b** on LPS-induced NO generation were evaluated in BV-2 microglial cells. The results showed that most of the novel synthetic compounds (using compound **2** and dehydroepiandrosterone (DHEA) as positive controls) exhibited modest to strong inhibitory activity on NO generation at 20 μM (Table 2). Meanwhile, the cytotoxicity of the compounds was determined by MTT assay to exclude the possibility that the reduced release of NO was caused by cytotoxic effects of the compounds (Table 2). The results showed that compounds with a double bond at C-16,17 exhibited moderate to strong inhibitory activity (**9b**, **15a**, **15b**, **16a**, **16b**, **18a**, and **18b**). The introduction of a CH$_3$ group at the C-16 position resulted in an increase inhibitory potency (**14a** > **10a**, **14b** > **10b**, **17a** > **13a**, and **17b** > **13b**). Obvious toxicity was observed for compounds **11a** and **11b**, in which R$_2$ was a benzyl group. In the case where the R$_3$ substituent was changed from C(CH$_3$)$_3$ to m-xylene, cytotoxicity was also increased (**16a**). A benzyl group for R$_1$ was effective, as compounds **12b**, **18a**, and **18b** all showed good inhibitory activity. It was difficult to determine the effects of the R/S configuration at R$_1$ on the biological activities. Generally, when C-16,17 was a double bond, the configuration of the compounds had a minimal impact on the inhibitory activities (**15a/15b**, **16a/16b**, and **18a/18b**), especially for **18a** and **18b**, which had very similar activities. However, it was different for **9a** and **9b**: **9b** was more potent than **9a** (R > S). Compounds **9b**, **10a**, **12b**, **13b**, **14a**, **15a**, **15b**, **18a**, and **18b**, which strongly suppressed LPS-induced NO generation and had low cytotoxicity in BV-2 microglia (cell viability >90%), were chosen for a concentration-dependent experiment in LPS-treated BV-2 microglia. Compounds **10a**, **14a**, **18a**, and **18b** were found to be the most potent, with IC$_{50}$ values of 12.4, 12.8, 14.3, and 8.5 μM, respectively (Figure 3).

Compound **18b** emerged as the most potent of all compounds tested. The structure of **18b** was determined by X-ray analysis of a single crystal of compound **18ax**, the p-nitrobenzoyl derivative of compound **18a**, because compounds **18a**, **18b**, and the p-nitrobenzoyl derivative of **18b** were difficult to crystallize (Scheme 2).

On the basis of its strong inhibitory activity on NO generation and minimal cytotoxicity to microglial cells, compound **18b** was selected for further evaluation. The

Scheme 1. Synthesis of Target Compounds 9a–18b[a]
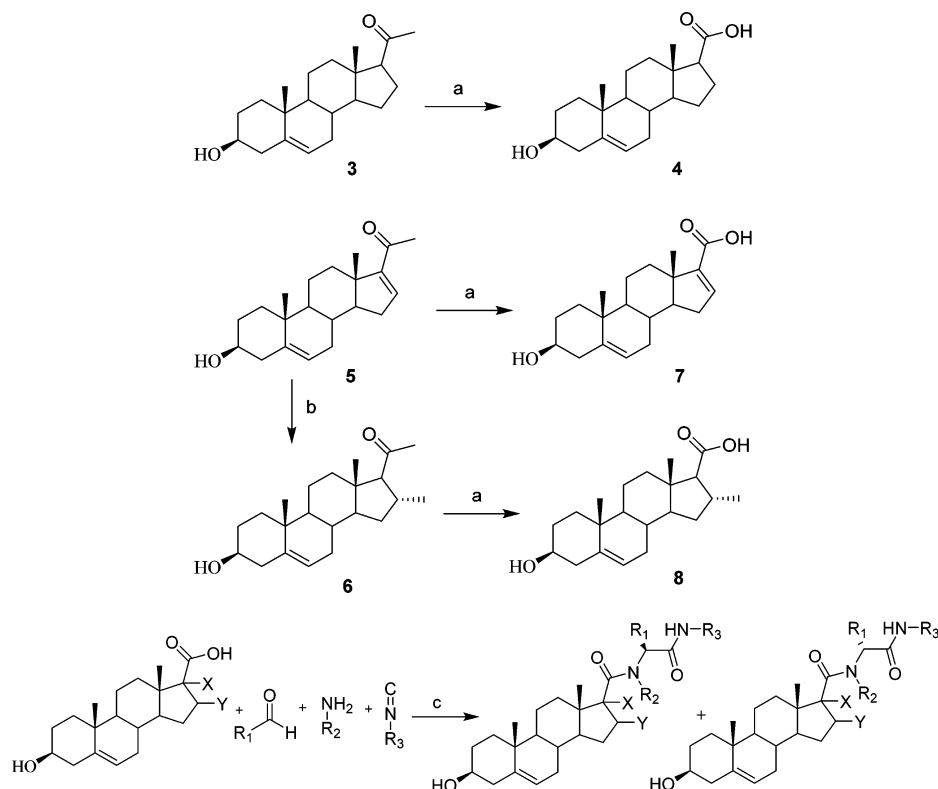
[a]Reagents and conditions: (a) NaOH, Br₂, dioxane/H₂O, −5 to 10 °C; (2) HCl, 90 °C; (b) MeMgI, CuCl, THF, −10 to 0 °C; (c) Sc(OTf)₃, MeOH, rt.
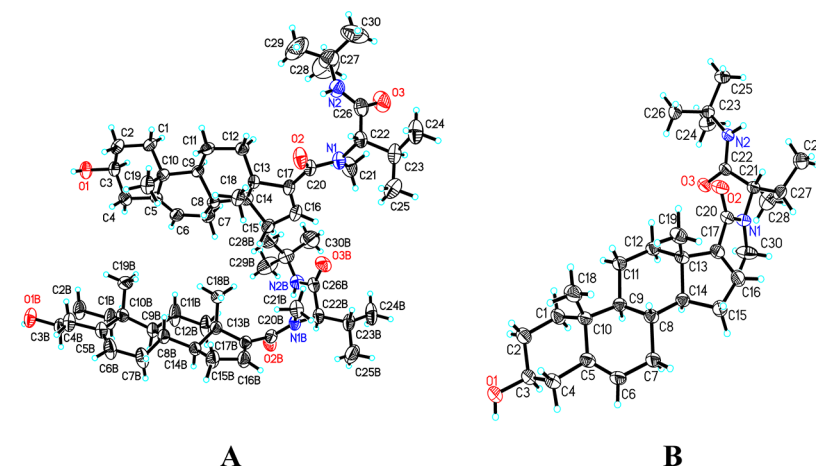

Figure 2. X-ray structure of the mixture of **9a** and **9b** (A); X-ray structure of **9a** (B).

dose–response study showed that compound **18b** significantly inhibited LPS-induced NO production in a dose-dependent manner in BV-2 microglial cells (Figure 4A). The effect of compound **18b** on LPS-induced NO generation was also examined in primary microglia, HAPI cells, and primary astrocytes stimulated with LPS or LPS/IFN-γ. The results showed that compound **18b** markedly suppressed LPS- or LPS/IFNγ-induced NO production in HAPI cells, primary microglia, and primary astrocytes (Figure 4B–D). These results indicate that the NO inhibitory effects of compound **18b** are widespread. Compound **18b** did not affect cell viability at the tested concentration (data not shown).

Together with NO, PGE-2 is also a well-known inflammatory mediator. The production of NO and PGE-2 is catalyzed by inducible NO synthase (iNOS) and cyclooxygenase-2 (COX-2), respectively, which are key neuroinflammatory enzymes in the brain's response to neurodegenerative processes.[15−17] Likewise, inflammatory cytokines, including IL-6, IL-1β, and TNF-α, are also secreted by activated microglial cells, which ultimately leads to neuronal cell damage and contributes to the progression of neurodegeneration.[18] Therefore, we tested whether compound **18b** inhibited the transcriptional expression of these cytokines and inflammatory enzymes using quantitative real-time (RT)-PCR analysis. The result showed that compound **18b** significantly inhibited the LPS-induced

Table 2. Inhibitory Activity of Compounds 9a–18b (20 μM) on NO Generation in LPS-Treated BV-2 Microglial Cells

compd	% inhibition	% cell viability	IC$_{50}$ (μM)
9a	31.77 ± 2.74	83.54 ± 2.84	
9b	**66.81 ± 5.21**	88.14 ± 3.30	21.398 ± 1.330
10a	**52.86 ± 3.69**	97.41 ± 1.04	**12.428 ± 1.094**
10b	20.31 ± 6.94	99.22 ± 1.35	
11a	56.51 ± 0.45	77.10 ± 4.8	
11b	45.57 ± 5.2	13.62 ± 1.57	
12a	10.42 ± 1.63	74.12 ± 1.55	
12b	**80.47 ± 2.09**	60.71 ± 4.86	17.265 ± 1.237
13a	15.09 ± 6.12	104.53 ± 1.76	
13b	**63.75 ± 5.18**	94.31 ± 4.75	16.189 ± 1.209
14a	**73.48 ± 6.58**	78.90 ± 2.62	**12.844 ± 1.109**
14b	45.99 ± 2.92	90.76 ± 5.16	
15a	**80.04 ± 7.17**	71.40 ± 3.0	14.181 ± 1.152
15b	**68.86 ± 5.94**	92.06 ± 3.71	17.411 ± 1.241
16a	68.84 ± 4.52	36.06 ± 3.17	
16b	74.24 ± 6.82	89.50 ± 4.66	
17a	28.18 ± 2.44	96.69 ± 4.00	
17b	83.33 ± 5.55	93.60 ± 3.07	
18a	**83.06 ± 2.81**	**92.05 ± 3.37**	**14.255 ± 1.154**
18b	**89.39 ± 6.94**	96.33 ± 5.88	**8.546 ± 0.932**
2	53.25 ± 3.57	101.37 ± 1.45	**18.347 ± 2.054**
DHEA	9.17 ± 2.98	101.26 ± 3.02	
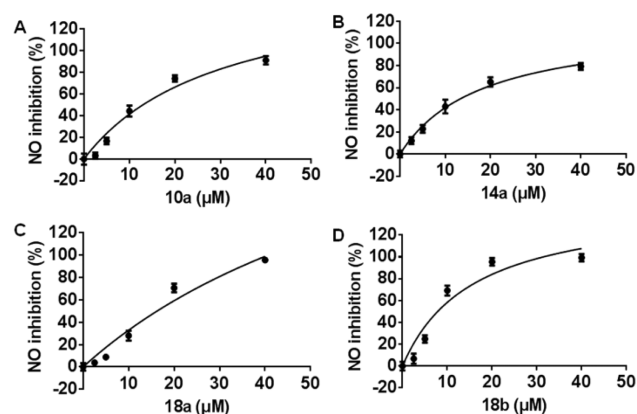
Figure 3. Concentration-dependent inhibition of NO production by compounds **10a**, **14a**, **18a**, and **18b** in LPS-activated microglial cells. BV-2 microglial cells were preincubated with the compound for 30 min prior to LPS (0.1 μg/mL) stimulation. The nitrite levels in the cell culture medium were detected using Griess reagents. Data shown are the mean ± SD for each group (n = 3) and are representative of three independent experiments.

expression of the genes for iNOS, TNF-α, IL-6, and COX-2 mRNA in a dose-dependent manner in BV-2 microglial cells (Figure 5A−D). We further examined the suppressive effects of compound **18b** on the production of iNOS, COX-2, TNF-α, IL-6, and PGE-2 at the protein level using western blot analysis or enzyme-linked immunosorbent assay (ELISA). Consistent with the quantitative RT-PCR data, compound **18b** significantly reduced the levels of these proteins in LPS-stimulated BV-2 microglial cells (Figure 6A−C). These results indicate that compound **18b** has a significant anti-inflammatory activity and might be a promising agent for the therapeutic treatment of neuroinflammatory disorders.

The transcription factor NF-κB regulates the expression of numerous inflammatory genes, such as iNOS, TNF-α, IL-6,

COX-2, and IL-1β, in activated microglial cells, and the inhibition of NF-κB activation may have anti-inflammatory and neuroprotective effects.[19] Therefore, the effect of compound **18b** on NF-κB activation in activated microglial cells was investigated. It is well-known that NF-κB activation is characterized by the phosphorylation of IKK and IκB and the subsequent degradation of IκB in the cytoplasm. After the nuclear translocation of NF-κB, the p65 subunit of NF-κB binds to a κB element of the promoter region, which ultimately controls the transcriptional expression of the target genes.[19]

As shown in Figure 7A, compound **18b** did not inhibit either the phosphorylation of IKK and IκB or the degradation of IκB. In addition, the nuclear translocation of the p65 subunit of NF-κB was not affected by compound **18b**, indicating that these upstream molecules of NF-κB are not the primary target for compound **18b** when acting as an anti-inflammatory agent (Figure 7B). Mitogen activated protein kinases (MAPKs) are also key regulators that mediate important biological processes and cellular responses to inflammatory stimulation.[20] There are three main subfamilies in mammals: extracellular signal-regulated kinase (ERK1/2), p38 MAPK, and c-jun N-terminal kinase (JNK). The activation of MAPKs modulates the transcriptional expression of diverse genes involved inflammatory responses. Thus, the effects of compound **18b** on the activation of MAPKs were investigated in LPS-activated BV-2 microglial cells. The results showed that the LPS-induced phosphorylation of p38 MAPK and JNK was significantly inhibited by compound **18b**, whereas the activation of ERK1/2 was not inhibited (Figure 7C). p38 MAPK and JNK regulate inflammatory gene expression by affecting transcription factors AP-1 and NF-κB in macrophages and microglial cells. Therefore, we tested the effect of compound **18b** on the LPS-induced activation of AP-1 and NF-κB in BV-2 microglial cells using a lentivirus-mediated luciferase activity assay. The results showed that compound **18b** significantly suppressed the transcriptional activity of AP-1 and NF-kB in LPS-stimulated BV-2 microglial cells (Figure 7D,E). These results suggest that the inhibition of the p38 MAPK and/or JNK signal transduction pathways and the subsequent suppression of AP-1 and/or NF-κB transcriptional activities might be involved in the anti-inflammatory mechanisms of compound **18b**.

Excessive activation of microglial cells produces high levels of neurotoxic factors, including free radicals and inflammatory cytokines, thereby leading to the damage or death of the surrounding neurons.[21] A compound that inhibits the production of free radicals and inflammatory cytokines by microglial cells may be neuroprotective. Indeed, many anti-inflammatory compounds demonstrate neuroprotective activity *in vitro* and *in vivo* by inhibiting microglial activation.[1,4] Therefore, the neuroprotective activities of compound **18b** were investigated using a microglia-conditioned medium (CM)/neuron coculture system. When HT-22 neuroblastoma cells were treated with LPS-activated microglial cell-derived CM, the viability of the HT-22 cells was significantly decreased. However, when the HT-22 cells were treated with CM collected from LPS-activated microglial cells that were pretreated with compound **18b**, the viability of the HT-22 cells was maintained (Figure 8A). To examine whether compound **18b** directly protects neurons against the cytotoxicity of oxidative stress, the effect of the compound on H$_2$O$_2$-induced HT-22 cell death was also checked. The results showed that compound **18b** did not prevent H$_2$O$_2$-induced HT-22 cell death (Figure 8B), suggesting that the neuroprotective activity

Scheme 2. Synthesis of the Derivative of Compound 18a[a]
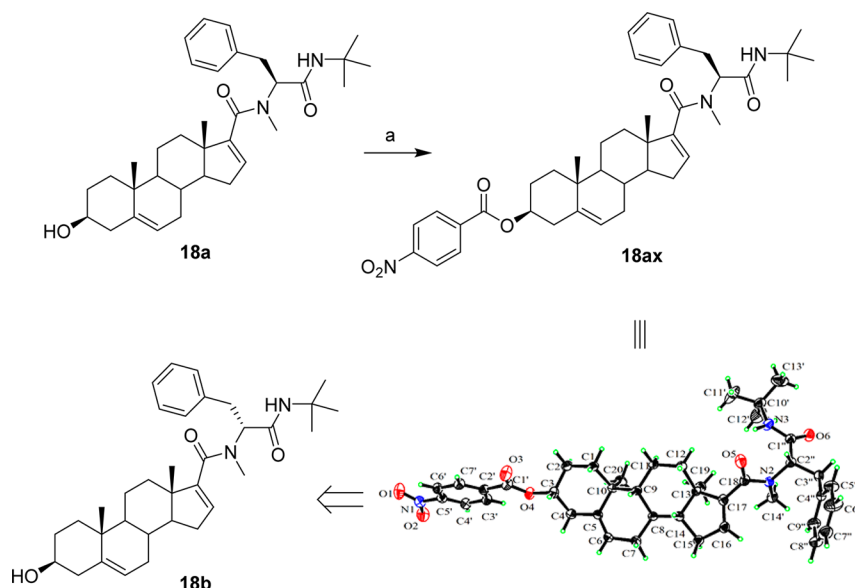
[a]Reagents and conditions: (a) p-nitrobenzoic acid, DCC, DMAP, CH$_2$Cl$_2$.

of compound **18b** is mainly attributable to the modulation of microglial activation.

Ischemic stroke is one of the leading causes of disability and is accompanied by significant microglial activation that plays an important role in the pathogenesis of neurodegenerative diseases. Because compound **18b** exhibited a strong anti-inflammatory activity *in vitro*, the therapeutic potential of compound **18b** was further investigated *in vivo* using a middle cerebral artery occlusion (MCAO) mouse model. Pretreatment of compound **18b** (40 mg/kg) markedly decreased the cortical (ischemic penumbra), hemispheric, and edema-corrected infarction volumes, whereas the striatum (ischemic core) infarction volume was not significantly affected (Figure 8C). These results are consistent with previous findings that have shown that, unlike in the ischemic core, the ischemic penumbra is a recoverable region and is most likely treatable with pharmacological interventions.[22,23] The expression of proinflammatory genes was also determined by quantitative RT-PCR analysis. The result showed that compound **18b** significantly inhibited the expression of TNF-α and IL-6 mRNAs in the MCAO mouse model (Figure 8D–G). In general, the *in vivo* efficacy of a compound is dependent on its pharmacokinetic nature in addition to its pharmacodynamic properties. In the current study, we did not test the pharmacokinetic properties of compound **18b**, **1**, or **2**. Although the IC$_{50}$ value may not completely reflect the efficacy of a compound *in vivo*, it partially reflects the potency of a compound in the mouse model. Moreover, the conclusion of the *in vivo* study also could not rule out the possibility that the neuroprotective properties of compound **18b** were due to its action on a peripheral system. Thus, future studies are required to test the pharmacokinetic nature (including blood−brain barrier studies) of compound **18b** and the neuroprotective effects of compounds **1** and **2** *in vivo*. Taken together, our results suggest that compound **18b** might be a potential agent for the prevention and/or treatment of ischemic stroke and other neurodegenerative diseases. This inhibition of microglial activation may be the underlying mechanism for the observed effects of compound **18b**.

■ CONCLUSIONS

In the present study, we efficiently synthesized a number of novel sterol derivatives with dipeptide-like side chains and found that compound **18b** exhibited the most potent activity in the inhibition of NO production and the expression of proinflammatory factors, including TNF-α, IL-6, and PGE-2. The anti-inflammatory effects of compound **18b** were likely through the inhibition of the MAPKs/AP-1 or NF-κB signal transduction pathways in activated microglial cells. Furthermore, *in vitro* and *in vivo* studies demonstrated that compound **18b** possesses potent neuroprotective activity via the suppression of microglial activation. Collectively, our results indicate that compound **18b** might be a potential therapeutic candidate for neuroinflammatory disorders.

■ METHODS

Chemistry. *General Procedure to Obtain Compounds 9a−18b.* The 17-carboxylic acid (**4**, **7**, or **8**; 0.1 mmol) was suspended in 1 mL of methanol, and 1.1 equiv of the corresponding amine, 1.1 equiv of the corresponding aldehyde, and 0.1 equiv of Sc(OTf)$_3$ were added. The mixture was stirred for 15 min at room temperature, and then 1.1 equiv of the isonitrile was added. The reaction was kept under the same conditions until the total disappearance of the acid occurred. The solvent was evaporated under reduced pressure, and the residue was collected in EtOAc and washed with NaOH (5% aq.). The compounds were purified by silica gel column chromatography (hexane/EtOAc gradient) or Pre-HPLC.

Characterization Data for Compounds 9a−18b. (3S,10R,13S)-N-((S)-1-(tert-Butylamino)-3-methyl-1-oxobutan-2-yl)-3-hydroxy-N,10,13-trimethyl-2,3,4,7,8,9,10,11,12,13,14,15-dodecahydro-1H-cyclopenta[a]phenanthrene-17-carboxamide (**9a**). [α]$_D^{20}$ = +56.000 (c 0.100, CHCl$_3$); ^{1}H NMR (400 MHz, acetone-d_6) δ 6.75 (s, 1H), 5.81 (s, 1H), 5.35 (d, J = 4.9 Hz, 1H), 4.44 (d, J = 10.8 Hz, 1H), 3.70 (d, J = 4.5 Hz, 1H), 3.46−3.34 (m, 1H), 2.97 (s, 3H), 1.32 (s, 9H), 1.06 (s, 6H), 0.95 (d, J = 6.4 Hz, 3H), 0.81 (d, J = 6.4 Hz, 3H); ^{13}C NMR (126 MHz, acetone-d_6) δ 205.51, 205.36, 205.20, 169.29, 169.04, 148.87, 141.84, 130.30, 120.41, 70.78, 70.66, 62.53, 56.71, 50.78, 50.44, 48.54, 42.47, 37.26, 36.67, 34.49, 32.17, 31.97, 31.63, 31.41, 30.27, 27.98, 25.32, 20.54, 19.09, 18.85, 18.01, 16.24. MS (EI, m/z) = 484 (M$^+$); HRMS (EI): calcd for C$_{30}$H$_{48}$N$_2$O$_3$, 484.3665; found, 484.3659.
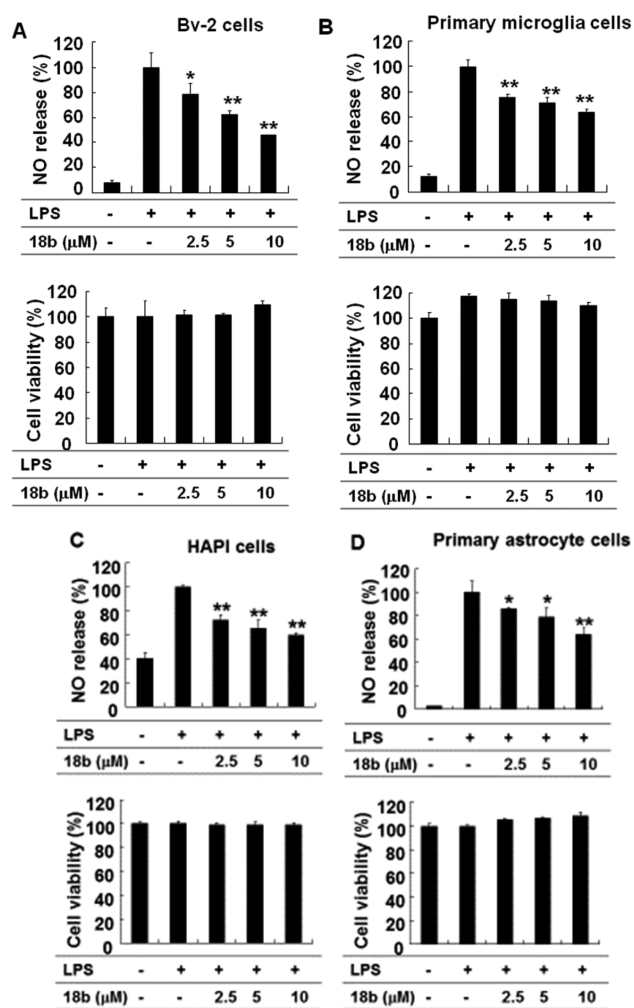
Figure 4. Compound **18b** inhibits LPS-induced NO production in microglial cells. Microglial cells were preincubated with compound **18b** for 30 min prior to LPS (0.1 μg/mL) or LPS (0.1 μg/mL)/IFN-γ (50 U/mL) stimulation: BV-2 microglia (A), primary microglia culture (B) HAPI microglia (C), and primary astrocytes (D). The nitrite levels in the cell culture medium were detected using Griess reagents (upper half of each panel). MTT assay was performed to assess cell viability (lower half of each panel). Data shown are the mean ± SD for each group ($n = 3$) and are representative of four independent experiments. Asterisks denote a significant difference from groups receiving LPS or LPS/IFN-γ treatment alone (*, $p < 0.05$; **, $p < 0.01$).

(3S,10R,13S)-N-(R)-(1-(tert-Butylamino)-3-methyl-1-oxobutan-2-yl)-3-hydroxy-N,10,13-trimethyl-2,3,4,7,8,9,10,11,12,13,14,15-dodecahydro-1H-cyclopenta[a]phenanthrene-17-carboxamide (9b). $[\alpha]_D^{20} = -249.375$ (c 0.160, CHCl$_3$); ^{1}H NMR (400 MHz, CDCl$_3$) δ 6.26 (s, 1H), 5.87 (s, 1H), 5.38 (s, 1H), 4.42 (d, $J = 10.6$ Hz, 1H), 3.62–3.43 (m, 1H), 2.96 (s, 3H), 1.30 (s, 9H), 1.12 (s, 3H), 1.05 (s, 3H), 0.97 (d, $J = 6.1$ Hz, 3H), 0.86 (d, $J = 6.4$ Hz, 3H); ^{13}C NMR (126 MHz, CDCl$_3$) δ 170.87, 169.22, 148.50, 141.23, 132.58, 121.16, 71.65, 62.70, 56.63, 50.97, 50.54, 48.70, 42.28, 37.21, 36.75, 34.07, 32.78, 32.42, 31.59, 30.20, 28.68, 25.19, 20.65, 19.84, 19.35, 18.54, 16.71; MS (EI, m/z) = 484 (M$^+$); HRMS (EI): calcd for C$_{30}$H$_{48}$N$_2$O$_3$, 484.3665; found, 484.3668.

(3S,10R,13S)-N-(−)-(1-(tert-Butylamino)-3-methyl-1-oxobutan-2-yl)-3-hydroxy-N,10,13-trimethyl-2,3,4,7,8,9,10,11,12,13,14,15,16,17-tetradecahydro-1H-cyclopenta[a]phenanthrene-17-carboxamide (10a). $[\alpha]_D^{20} = -130.588$ (c 0.085, CHCl$_3$); ^{1}H NMR (400 MHz, CDCl$_3$) δ 6.03 (s, 1H), 5.35 (d, $J = 5.0$ Hz, 1H), 4.52 (d, $J = 10.9$ Hz, 1H), 3.59–3.45 (m, 1H), 2.99 (s, 3H), 2.73 (t, $J = 8.8$ Hz, 1H), 2.35–2.13 (m, 5H), 1.30 (s, 9H), 1.01 (s, 3H), 0.94 (d, $J = 6.4$ Hz, 3H), 0.78

(s, 3H), 0.77 (d, $J = 6.6$ Hz, 3H); ^{13}C NMR (126 MHz, CDCl$_3$) δ 174.73, 169.59, 140.69, 121.29, 71.57, 56.54, 51.32, 50.87, 49.91, 45.54, 42.12, 39.32, 37.15, 36.44, 31.91, 31.79, 31.49, 28.59, 25.91, 25.00, 24.73, 20.88, 19.65, 19.31, 18.35, 14.04; MS (ESI, m/z) = 509.5 [M + 23]$^+$; HRMS (ESI): calcd for C$_{30}$H$_{50}$N$_2$O$_3$Na, 509.3719; found, 509.3709.

(3S,10R,13S)-N-(+)-(1-(tert-Butylamino)-3-methyl-1-oxobutan-2-yl)-3-hydroxy-N,10,13-trimethyl-2,3,4,7,8,9,10,11,12,13,14,15,16,17-tetradecahydro-1H-cyclopenta[a]phenanthrene-17-carboxamide (10b). $[\alpha]_D^{20} = +78.750$ (c 0.160, acetone-d_6); ^{1}H NMR (400 MHz, acetone-d_6) δ 6.15 (s, 1H), 5.35 (d, $J = 5.2$ Hz, 1H), 4.42 (d, $J = 10.7$ Hz, 1H), 3.58–3.46 (m, 1H), 2.98 (s, 3H), 2.77 (t, $J = 8.9$ Hz, 1H), 2.37–2.15 (m, 5H), 1.28 (s, 10H), 1.00 (s, 3H), 0.95 (d, $J = 6.4$ Hz, 3H), 0.84 (d, $J = 6.6$ Hz, 3H), 0.72 (s, 3H); ^{13}C NMR (126 MHz, CDCl$_3$) δ 175.07, 169.57, 140.66, 121.32, 71.57, 56.63, 51.46, 50.88, 49.97, 45.35, 42.14, 38.93, 37.17, 36.44, 31.90, 31.77, 31.51, 28.57, 25.33, 25.29, 24.67, 21.00, 19.67, 19.29, 18.83, 13.68; MS (ESI, m/z) = 509.5 [M + 23]$^+$; HRMS (ESI): calcd for C$_{30}$H$_{50}$N$_2$O$_3$Na, 509.3719; found, 509.3706.

(3S,10R,13S)-N-Benzyl-N-(−)-(1-(tert-butylamino)-3-methyl-1-oxobutan-2-yl)-3-hydroxy-10,13-dimethyl-2,3,4,7,8,9,10,11,12,13,-14,15,16,17-tetradecahydro-1H-cyclopenta[a]phenanthrene-17-carboxamide (11a). $[\alpha]_D^{20} = -88.333$ (c 0.180, CHCl$_3$); ^{1}H NMR (400 MHz, CDCl$_3$) δ 7.40–7.09 (m, 6H), 5.32 (s, 1H), 4.95 (d, $J = 17.9$ Hz, 1H), 4.64 (d, $J = 18.5$ Hz, 1H), 4.22 (s, 1H), 3.49 (s, 1H), 2.63 (t, $J = 9.0$ Hz, 1H), 2.34–2.11 (m, 3H), 1.30 (s, 9H), 1.00 (s, 4H), 0.90 (d, $J = 6.4$ Hz, 3H), 0.86 (s, 3H), 0.71 (d, $J = 6.0$ Hz, 3H); ^{13}C NMR (126 MHz, CDCl$_3$) δ 176.54, 170.21, 140.77, 138.03, 128.55, 127.20, 126.39, 121.37, 71.64, 56.40, 52.58, 51.00, 49.92, 45.73, 42.21, 38.92, 37.23, 36.54, 31.90, 31.81, 31.58, 28.64, 27.06, 26.70, 24.80, 20.86, 19.93, 19.86, 19.40, 14.19; MS (EI, m/z) = 562 (M$^+$); HRMS (EI): calcd for C$_{36}$H$_{54}$N$_2$O$_3$, 562.4134; found, 562.4131.

(3S,10R,13S)-N-Benzyl-N-(1-(tert-butylamino)-3-methyl-1-oxobutan-2-yl)-3-hydroxy-10,13-dimethyl-2,3,4,7,8,9,10,11,12,13,-14,15,16,17-tetradecahydro-1H-cyclopenta[a]phenanthrene-17-carboxamide (11b). $[\alpha]_D^{20} = -28.095$ (c 0.210, CHCl$_3$); ^{1}H NMR (400 MHz, CDCl$_3$) δ 7.32–7.13 (m, 3H), 7.05 (d, $J = 7.6$ Hz, 2H), 6.28 (s, 1H), 5.31 (s, 1H), 4.73 (dd, $J = 54.3, 17.3$ Hz, 2H), 4.47 (s, 1H), 3.50 (s, 1H), 2.53 (t, $J = 8.9$ Hz, 1H), 1.20 (s, 9H), 1.00 (s, 3H), 0.94 (d, $J = 6.3$ Hz, 3H), 0.88 (d, $J = 6.3$ Hz, 3H), 0.77 (s, 3H); ^{13}C NMR (126 MHz, CDCl$_3$) δ 176.31, 169.05, 140.69, 138.24, 128.44, 126.89, 125.92, 121.45, 71.68, 56.51, 52.83, 51.14, 49.96, 45.70, 42.23, 39.16, 37.27, 36.54, 31.93, 31.79, 31.61, 28.54, 26.99, 26.36, 24.73, 21.10, 19.74, 19.39, 19.17, 14.07; MS (EI, m/z) = 562 (M$^+$); HRMS (EI): calcd for C$_{36}$H$_{54}$N$_2$O$_3$, 562.4134; found, 562.4142.

(3S,10R,13S)-N-(+)-(1-(tert-Butylamino)-1-oxo-3-phenylpropan-2-yl)-3-hydroxy-N,10,13-trimethyl-2,3,4,7,8,9,10,11,12,13,14,-15,16,17-tetradecahydro-1H-cyclopenta[a]phenanthrene-17-carboxamide (12a). $[\alpha]_D^{20} = +79.335$ (c 0.155, CHCl$_3$); ^{1}H NMR (300 MHz, CDCl$_3$) δ 7.29–7.06 (m, 5H), 6.29 (s, 1H), 5.40 (dd, $J = 11.0, 5.6$ Hz, 1H), 5.34–5.27 (m, 1H), 3.60–3.40 (m, 1H), 3.17 (dd, $J = 15.1, 5.7$ Hz, 1H), 2.87 (s, 3H), 2.58 (t, $J = 8.8$ Hz, 1H), 2.34–2.09 (m, 3H), 1.29 (s, 10H), 0.97 (s, 3H), 0.37 (s, 3H); ^{13}C NMR (126 MHz, CDCl$_3$) δ 175.28, 169.94, 140.78, 137.43, 129.09, 128.51, 126.41, 121.38, 71.70, 57.80, 56.69, 51.48, 50.98, 50.01, 45.15, 42.23, 37.75, 37.22, 36.48, 33.52, 31.97, 31.86, 31.59, 31.39, 28.71, 25.04, 24.65, 20.73, 19.36, 12.98; MS (EI, m/z) = 534 (M$^+$); HRMS (EI): calcd for C$_{34}$H$_{50}$N$_2$O$_3$, 534.3821; found, 534.3825.

(3S,10R,13S)-N-(−)-(1-(tert-Butylamino)-1-oxo-3-phenylpropan-2-yl)-3-hydroxy-N,10,13-trimethyl-2,3,4,7,8,9,10,11,12,13,-14,15,16,17-tetradecahydro-1H-cyclopenta[a]phenanthrene-17-carboxamide (12b). $[\alpha]_D^{20} = -108.889$ (c 0.090, CHCl$_3$); ^{1}H NMR (300 MHz, CDCl$_3$) δ 7.32–7.11 (m, 5H), 6.03 (s, 1H), 5.47–5.21 (m, 2H), 3.59–3.40 (m, 1H), 3.28 (dd, $J = 14.5, 8.1$ Hz, 1H), 2.96 (s, 3H), 2.89 (dd, $J = 14.1, 9.3$ Hz, 1H), 2.60 (t, $J = 9.3$ Hz, 1H), 2.37–1.92 (m, 4H), 1.28 (s, 9H), 1.01 (s, 3H), 0.78 (s, 3H); ^{13}C NMR (126 MHz, CDCl$_3$) δ 174.72, 169.62, 140.75, 137.51, 128.95, 128.36, 126.41, 121.42, 71.69, 57.10, 56.64, 51.30, 51.01, 50.03, 45.51, 42.23, 39.44, 37.26, 36.54, 33.37, 31.98, 31.88, 31.60, 30.96, 28.68, 25.94, 24.76, 21.01, 19.42, 14.17; MS (EI, m/z) = 534 (M$^+$); HRMS (EI): calcd for C$_{34}$H$_{50}$N$_2$O$_3$, 534.3821; found, 534.3827.
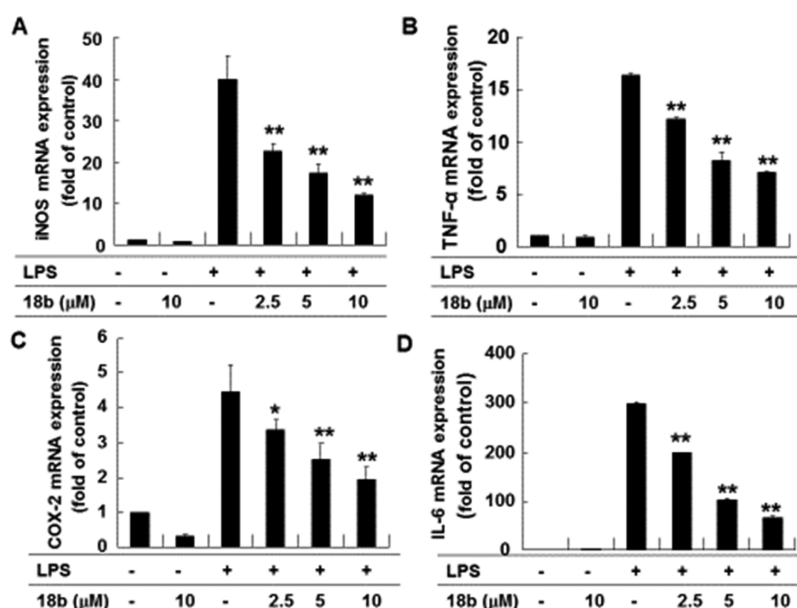
Figure 5. Compound **18b** inhibits LPS-induced inflammatory gene expression at the transcriptional level in BV-2 microglial cells. Cells were preincubated with compound **18b** for 30 min prior to LPS (0.1 μg/mL) stimulation. After treatment with LPS for 6 h, the mRNA level of iNOS (A), TNF-α (B), COX-2 (C), and IL-6 (D) was assessed by SYBR Green quantitative RT-PCR. Data shown are the mean $\pm$ SD of three independent experiments. Asterisks denote a significant difference from the group receiving LPS treatment alone (*, $p < 0.05$; **, $p < 0.01$).
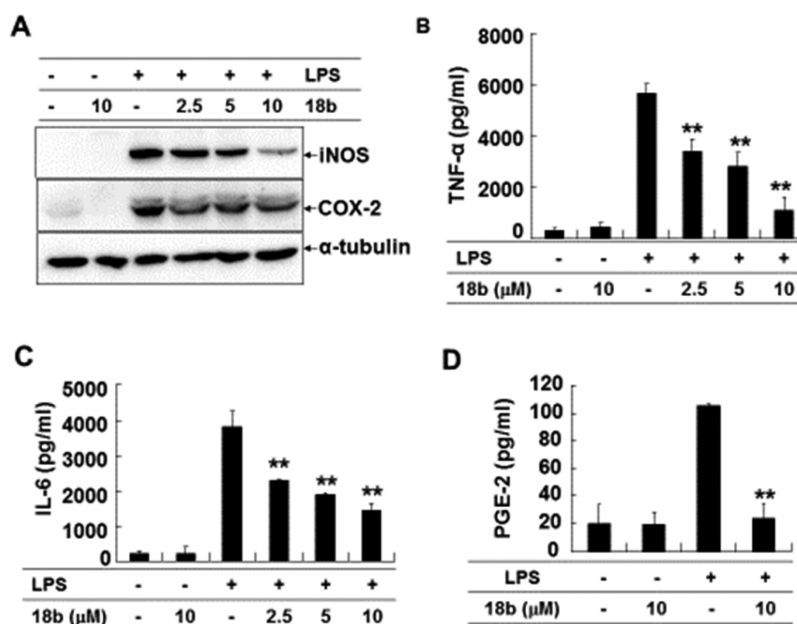

Figure 6. Compound **18b** inhibits LPS-induced inflammatory gene expression at the protein level in BV-2 microglial cells. Cells were preincubated with compound **18b** for 30 min prior to LPS stimulation. After treatment with LPS (0.1 μg/mL) for 16 h, total protein was extracted and subjected to western blot analysis to detect the iNOS and COX-2 proteins (A). Data shown are representative of three independent experiments. After treatment with LPS for 16 h, cell culture medium was collected and an ELISA was performed to assess the levels of TNF-α (B), IL-6 (C), and PGE-2 (D). Data shown are the mean $\pm$ SD for each group ($n = 3$) and are representative of three independent experiments. Asterisks denote a significant difference from the group receiving LPS treatment alone (*, $p < 0.05$; **, $p < 0.01$).

(3S,10R,13S)-N-(−)-(2-(tert-Butylamino)-2-oxo-1-phenylethyl)-3-hydroxy-N,10,13-trimethyl-2,3,4,7,8,9,10,11,12,13,14,15,16,17-tetradecahydro-1H-cyclopenta[a]phenanthrene-17-carboxamide (13a). $[\alpha]_D^{20} = -80.000$ (c 0.060, CHCl$_3$); ^{1}H NMR (300 MHz, CDCl$_3$) δ 7.41−7.27 (m, 5H), 6.14 (s, 1H), 5.71 (s, 1H), 5.35 (d, $J = 5.0$ Hz, 1H), 3.58−3.44 (m, 1H), 2.90 (s, 3H), 2.82 (t, $J = 8.7$ Hz, 1H), 1.36 (s, 9H), 1.01 (s, 3H), 0.78 (s, 3H); ^{13}C NMR (126 MHz, CDCl$_3$) δ 174.62, 169.34, 140.70, 136.26, 128.98, 128.76, 127.99, 121.53, 71.71, 61.25, 56.65, 51.62, 51.43, 50.08, 45.60, 42.26, 39.15, 37.27, 36.55, 33.45, 32.05, 31.90, 31.62, 29.73, 28.71, 26.93, 25.49, 24.80, 21.14,

19.41, 14.05; MS (EI, m/z) = 520 (M$^+$); HRMS (EI): calcd for C$_{33}$H$_{48}$N$_2$O$_3$, 520.3665; found, 520.3669.

(3S,10R,13S)-N-(+)-(2-(tert-Butylamino)-2-oxo-1-phenylethyl)-3-hydroxy-N,10,13-trimethyl-2,3,4,7,8,9,10,11,12,13,14,15,16,17-tetradecahydro-1H-cyclopenta[a]phenanthrene-17-carboxamide (13b). $[\alpha]_D^{20} = +2.727$ (c 0.110, CHCl$_3$); ^{1}H NMR (300 MHz, CDCl$_3$) δ 7.42−7.28 (m, 6H), 6.24 (s, 1H), 5.66 (s, 1H), 5.35 (d, $J = 5.4$ Hz, 1H), 3.60−3.43 (m, 1H), 2.89 (s, 3H), 2.78 (t, $J = 9.0$ Hz, 1H), 1.36 (s, 11H), 1.02 (s, 3H), 0.79 (s, 3H); ^{13}C NMR (126 MHz, CDCl$_3$) δ 174.55, 169.24, 140.85, 135.61, 129.39, 128.65, 128.03, 121.43, 71.73,
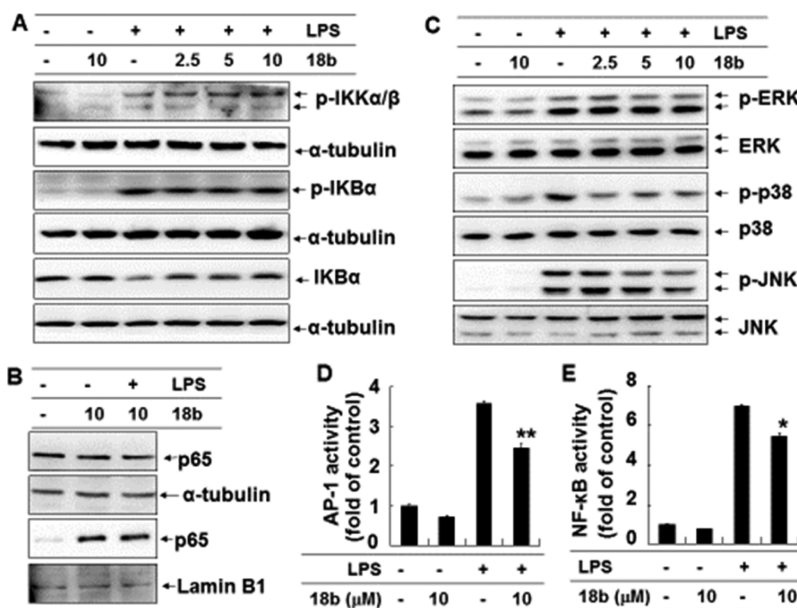
Figure 7. Compound **18b** suppressed LPS-induced MAPK activation and the subsequent activation of AP-1 and NF-κB in BV-2 microglial cells. Cells were pretreated with compound **18b** for 30 min prior to LPS (0.1 μg/mL) stimulation. After treatment with LPS for the indicated times, total protein was extracted. The phosphorylation of IKKα/β (10 min) and IκB-α (20 min) and degradation of IκB-α (30 min) were assessed by western blot analysis (A), as was the nuclear translocation of the p65 subunit of NF-κB (B). After stimulation with LPS for 30 min, the phosphorylation of ERK, JNK, and p38 were assessed by immunoblot analysis (C). BV-2 cells that expressed AP-1 (D) or NF-κB (E) lentiviral vectors were pretreated with compound **18b** prior to LPS stimulation for 30 min. After stimulation with LPS for 16 h, the total protein was extracted and luciferase activity was determined. Asterisks denote a significant difference from the group receiving LPS treatment alone (*, $p < 0.05$; **, $p < 0.01$).

60.91, 56.73, 51.52, 50.08, 45.80, 42.26, 39.29, 37.29, 36.58, 32.88, 32.06, 31.94, 31.63, 29.73, 28.67, 26.93, 25.74, 24.89, 21.14, 19.42, 13.88; MS (EI, m/z) = 520 (M$^+$); HRMS (EI): calcd for C$_{33}$H$_{48}$N$_2$O$_3$, 520.3665; found, 520.3661.

(3S,10R,13S,16R)-N-(−)-(1-(tert-Butylamino)-3-methyl-1-oxobutan-2-yl)-3-hydroxy-N,10,13,16-tetramethyl-2,3,4,7,8,9,10,11,12,-13,14,15,16,17-tetradecahydro-1H-cyclopenta[a]phenanthrene-17-carboxamide (14a). $[\alpha]_D^{20}$ = −140.000 (c 0.225, CHCl$_3$); ^{1}H NMR (300 MHz, CDCl$_3$) δ 6.09 (s, 1H), 5.34 (s, 1H), 4.53 (d, J = 11.1 Hz, 1H), 3.63−3.41 (m, 1H), 2.97 (s, 3H), 2.83−2.60 (m, 1H), 1.29 (s, 9H), 1.00 (s, 3H), 0.93 (d, J = 6.6 Hz, 6H), 0.82 (s, 3H), 0.77 (d, J = 6.5 Hz, 3H); ^{13}C NMR (126 MHz, CDCl$_3$) δ 174.11, 169.27, 140.39, 120.90, 71.17, 60.65, 55.02, 50.50, 49.69, 46.45, 41.77, 39.02, 36.80, 36.13, 34.38, 32.94, 31.38, 31.13, 28.26, 24.52, 21.24, 20.39, 19.26, 18.96, 17.91, 14.31; MS (EI, m/z) = 500 (M$^+$); HRMS (EI): calcd for C$_{31}$H$_{52}$N$_2$O$_3$, 500.3978; found, 500.3973.

(3S,10R,13S,16R)-N-(+)-(1-(tert-Butylamino)-3-methyl-1-oxobutan-2-yl)-3-hydroxy-N,10,13,16-tetramethyl-2,3,4,7,8,9,10,11,12,-13,14,15,16,17-tetradecahydro-1H-cyclopenta[a]phenanthrene-17-carboxamide (14b). $[\alpha]_D^{20}$ = +74.815 (c 0.270, CHCl$_3$); ^{1}H NMR (300 MHz, CDCl$_3$) δ 6.20 (s, 1H), 5.35 (s, 1H), 4.48 (d, J = 11.1 Hz, 1H), 3.69−3.39 (m, 1H), 2.95 (s, 3H), 2.89−2.66 (m, 1H), 2.35 (d, J = 8.9 Hz, 1H), 1.27 (s, 9H), 0.99 (s, 3H), 0.96 (d, J = 4.2 Hz, 3H), 0.93 (d, J = 4.7 Hz, 3H), 0.81 (d, J = 6.6 Hz, 3H), 0.76 (s, 3H); ^{13}C NMR (126 MHz, CDCl$_3$) δ 174.40, 169.16, 140.35, 120.96, 71.22, 60.74, 55.10, 50.44, 49.75, 46.31, 41.80, 38.53, 36.81, 36.13, 33.69, 32.77, 31.41, 31.34, 31.16, 28.25, 24.66, 21.32, 20.49, 19.35, 18.94, 18.33, 13.86; MS (EI, m/z) = 500 (M$^+$); HRMS (EI): calcd for C$_{31}$H$_{52}$N$_2$O$_3$, 500.3978; found, 500.3977.

(3S,10R,13S)-N-(+)-(2-(tert-Butylamino)-1-cyclohexyl-2-oxoethyl)-3-hydroxy-N,10,13-trimethyl-2,3,4,7,8,9,10,11,12,13,14,15-dodecahydro-1H-cyclopenta[a]phenanthrene-17-carboxamide (15a). $[\alpha]_D^{20}$ = +40.000 (c 0.395, CHCl$_3$); ^{1}H NMR (300 MHz, CDCl$_3$) δ 6.12 (s, 1H), 5.75 (s, 1H), 5.35 (d, J = 3.7 Hz, 1H), 4.51 (d, J = 10.6 Hz, 1H), 3.58−3.42 (m, 1H), 2.94 (s, 3H), 1.30 (s, 9H), 1.04 (s, 6H); ^{13}C NMR (126 MHz, CDCl$_3$) δ 170.03, 168.57, 148.32, 140.74, 130.00, 120.68, 71.17, 56.37, 50.68, 50.08, 48.46, 41.80, 36.71, 36.27, 33.99, 33.74, 31.89, 31.13, 31.10, 29.82, 29.59, 28.24, 28.14, 25.91,

25.23, 25.17, 20.25, 18.87, 16.34; MS (EI, m/z) = 524 (M$^+$); HRMS (EI): calcd for C$_{33}$H$_{52}$N$_2$O$_3$, 524.3978; found, 524.3970.

(3S,10R,13S)-N-(−)-(2-(tert-Butylamino)-1-cyclohexyl-2-oxoethyl)-3-hydroxy-N,10,13-trimethyl-2,3,4,7,8,9,10,11,12,13,14,15-dodecahydro-1H-cyclopenta[a]phenanthrene-17-carboxamide (15b). $[\alpha]_D^{20}$ = −182.353 (c 0.255, CHCl$_3$); ^{1}H NMR (300 MHz, CDCl$_3$) δ 6.29 (s, 1H), 5.84 (d, J = 1.5 Hz, 1H), 5.35 (d, J = 4.8 Hz, 1H), 4.50 (d, J = 11.2 Hz, 1H), 3.59−3.42 (m, 1H), 2.94 (s, 3H), 1.28 (s, 9H), 1.09 (s, 3H), 1.04 (s, 3H); ^{13}C NMR (126 MHz, CDCl$_3$) δ 170.37, 168.63, 148.04, 140.75, 131.93, 120.67, 71.16, 56.15, 50.53, 50.07, 48.23, 41.79, 36.73, 36.27, 33.84, 33.59, 32.41, 31.93, 31.11, 29.73, 29.69, 28.36, 28.21, 25.97, 25.22, 25.17, 20.18, 18.87, 16.24; MS (EI, m/z) = 524 (M$^+$); HRMS (EI): calcd for C$_{33}$H$_{52}$N$_2$O$_3$, 524.3978; found, 524.3980.

(3S,10R,13S)-N-(+)-(1-((2,6-Dimethylphenyl)amino)-3-methyl-1-oxobutan-2-yl)-3-hydroxy-N,10,13-trimethyl-2,3,4,7,8,9,10,11,12,-13,14,15-dodecahydro-1H-cyclopenta[a]phenanthrene-17-carboxamide (16a). $[\alpha]_D^{20}$ = +98.000 (c 0.150, CHCl$_3$); ^{1}H NMR (300 MHz, CDCl$_3$) δ 7.12−6.97 (m, 3H), 5.82 (s, 1H), 5.37 (d, J = 5.3 Hz, 1H), 3.61−3.40 (m, 1H), 3.05 (s, 3H), 2.19 (s, 6H), 1.09 (d, J = 6.4 Hz, 3H), 1.06 (s, 3H), 1.05 (s, 3H), 0.92 (d, J = 6.6 Hz, 3H); ^{13}C NMR (126 MHz, CDCl$_3$) δ 170.88, 168.09, 148.83, 141.18, 135.17, 133.65, 131.30, 128.14, 127.27, 121.19, 71.70, 56.91, 50.50, 49.00, 42.26, 37.17, 36.74, 34.49, 32.44, 31.61, 31.57, 30.32, 29.74, 25.06, 20.75, 19.78, 19.37, 18.55, 18.47, 16.84; MS (EI, m/z) = 532 (M$^+$); HRMS (EI): calcd for C$_{34}$H$_{48}$N$_2$O$_3$, 532.3665; found, 532.3663.

(3S,10R,13S)-N-(−)-(1-((2,6-Dimethylphenyl)amino)-3-methyl-1-oxobutan-2-yl)-3-hydroxy-N,10,13-trimethyl-2,3,4,7,8,9,10,11,12,-13,14,15-dodecahydro-1H-cyclopenta[a]phenanthrene-17-carboxamide (16b). $[\alpha]_D^{20}$ = −244.375 (c 0.160, CHCl$_3$); ^{1}H NMR (300 MHz, CDCl$_3$) δ 7.84 (s, 1H), 7.13−6.97 (m, 3H), 6.00 (s, 1H), 5.37 (d, J = 4.5 Hz, 1H), 4.69 (d, J = 11.2 Hz, 1H), 3.62−3.45 (m, 1H), 3.06 (s, 3H), 2.17 (s, 6H), 1.13 (s, 3H), 1.08 (d, J = 6.5 Hz, 3H), 1.05 (s, 3H), 0.95 (d, J = 6.6 Hz, 3H); ^{13}C NMR (126 MHz, CDCl$_3$) δ 171.10, 168.18, 148.35, 141.22, 135.27, 134.88, 133.73, 128.08, 127.21, 121.17, 71.70, 56.50, 50.47, 48.46, 42.26, 37.18, 36.74, 34.36, 32.51, 31.61, 31.58, 30.19, 29.73, 25.45, 20.67, 19.88, 19.36, 18.58, 16.74, 0.04; MS (EI, m/z) = 532 (M$^+$); HRMS (EI): calcd for C$_{34}$H$_{48}$N$_2$O$_3$, 532.3665; found, 532.3660.
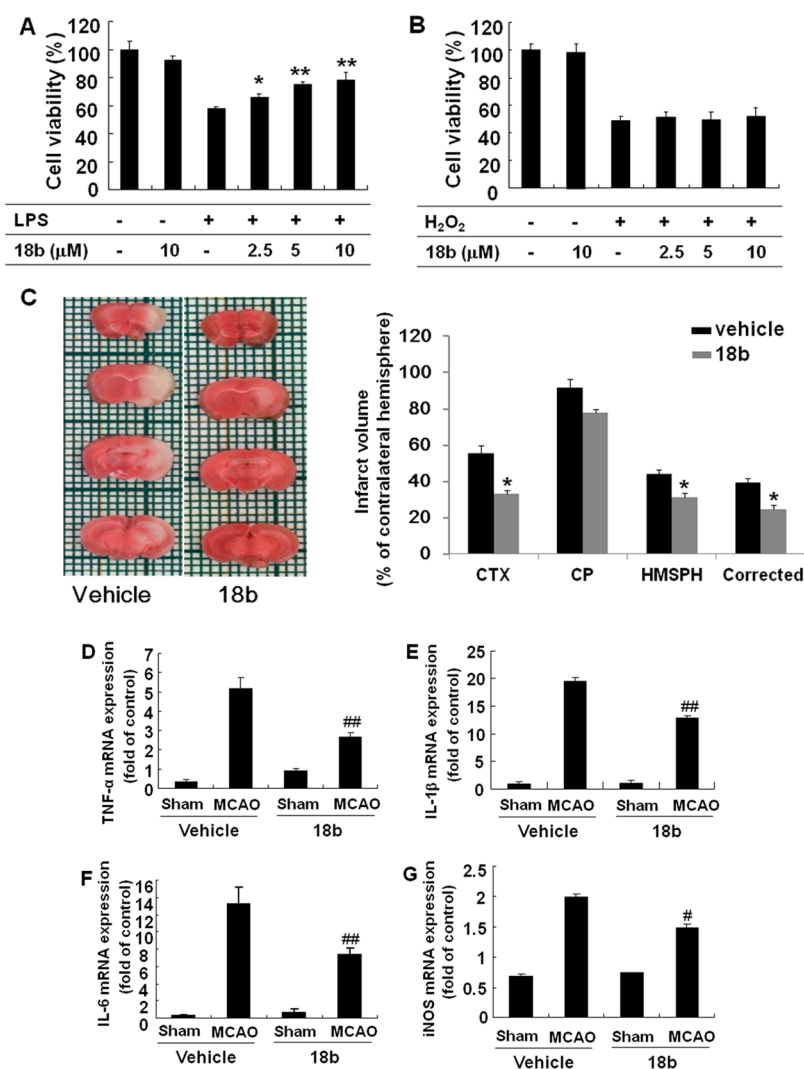
Figure 8. Compound **18b** reduced microglial neurotoxicity *in vitro* and *in vivo*. BV-2 microglial cells were pretreated with compound **18b** prior to LPS (0.1 μg/mL) stimulation for 30 min. After stimulation with LPS for 24 h, the CM from each group was collected. HT-22 cells were treated with the CM for 36 h, and an MTT assay was performed to assess cell viability (A). HT-22 cells were pretreated with compound **18b** for 30 min followed by treatment with H_2O_2 (0.5 mM). After treatment with H_2O_2 for 24 h, HT-22 cell viability was detected by MTT assay (B). Compound **18b** (40 mg/kg) was administered for 1 h prior to MCAO by intraperitoneal injection. After 24 h of reperfusion, the brain slices were stained with TTC (left) and the infarct volume was quantified (right) (C). CTX, cortex; CP, striatum; HEMI, hemisphere; CORRECT, hemisphere infarction corrected for edema. After 24 h of reperfusion, the mRNA levels of TNF-α (D), IL-1β (E), IL-6 (F), and iNOS (G) were assessed by SYBR Green quantitative RT-PCR. For the *in vitro* experiment, data shown are the mean ± SD for each group ($n = 3$) and are representative of three independent experiments. Asterisks denote a significant difference from the group receiving LPS treatment alone (*, $p < 0.05$; **, $p < 0.01$). For the *in vivo* study, data shown are the mean ± SD for each group ($n = 4$). Asterisks denote a significant difference from the group receiving the vehicle treatment alone (*, $p < 0.05$). Number signs indicate a significant difference from the vehicle-treated MCAO groups (#, $p < 0.05$; ##, $p < 0.05$).

(3S,10R,13S,16R)-N-(−)-(2-(tert-Butylamino)-2-oxo-1-phenyleth-yl)-3-hydroxy-N,10,13,16-tetramethyl-2,3,4,7,8,9,10,11,12,13,14,-15,16,17-tetradecahydro-1H-cyclopenta[a]phenanthrene-17-car-boxamide (17a). $[\alpha]_D^{20} = -131.667$ (*c* 0.060, CHCl₃); ¹H NMR (300 MHz, CDCl₃) δ 7.42−7.28 (m, 5H), 6.16 (s, 1H), 5.81 (s, 1H), 5.35 (d, *J* = 5.2 Hz, 1H), 3.57−3.44 (m, 1H), 2.91 (s, 3H), 2.42 (d, *J* = 8.5 Hz, 1H), 1.35 (s, 9H), 1.01 (s, 3H), 1.00 (d, *J* = 6.6 Hz, 3H), 0.84 (s, 3H); ¹³C NMR (126 MHz, CDCl₃) δ 174.48, 169.00, 140.72, 135.98, 128.86, 128.68, 127.87, 121.51, 71.70, 61.20, 60.98, 55.49, 51.51, 50.17, 46.94, 42.25, 39.09, 37.23, 36.58, 34.29, 33.50, 33.35, 31.87, 31.81, 31.60, 28.68, 21.95, 20.95, 19.42, 14.54; MS (EI, *m/z*) = 534 (M⁺); HRMS (EI): calcd for C₃₄H₅₀N₂O₃, 534.3821; found, 534.3829.

(3S,10R,13S,16R)-N-(2-(tert-Butylamino)-2-oxo-1-phenyelethyl)-3-hydroxy-N,10,13,16-tetramethyl-2,3,4,7,8,9,10,11,12,13,14,15,-16,17-tetradecahydro-1H-cyclopenta[a]phenanthrene-17-carboxa-mide (17b). $[\alpha]_D^{20} = -22.000$ (*c* 0.100, CHCl₃); ¹H NMR (300 MHz, CDCl₃) δ 7.40−7.29 (m, 5H), 6.27 (s, 1H), 5.73 (s, 1H), 5.35 (d, *J* = 5.1 Hz, 1H), 3.59−3.45 (m, 1H), 2.89 (s, 3H), 2.37 (d, *J* = 8.8 Hz, 1H), 1.36 (s, 9H), 1.01 (s, 3H), 0.97 (d, *J* = 6.9 Hz, 3H), 0.84 (s, 3H); ¹³C NMR (126 MHz, CDCl₃) δ 174.30, 169.14, 140.83, 135.68, 129.14, 128.67, 127.96, 121.44, 71.73, 61.10, 60.82, 55.46, 51.52, 50.16, 47.13, 42.24, 39.31, 37.25, 36.60, 34.41, 33.49, 33.00, 31.86, 31.61, 28.68, 22.05, 20.95, 19.43, 14.51; MS (EI, *m/z*) = 534 (M⁺); HRMS (EI): calcd for C₃₄H₅₀N₂O₃, 534.3821; found, 534.3817.

(3S,10R,13S)-N-((S)-1-(tert-Butylamino)-1-oxo-3-phenylpropan-2-yl)-3-hydroxy-N,10,13-trimethyl-2,3,4,7,8,9,10,11,12,13,14,15-do-decahydro-1H-cyclopenta[a]phenanthrene-17-carboxamide (18a). $[\alpha]_D^{20} = +9.722$ (*c* 0.360, CHCl₃); ¹H NMR (300 MHz, CDCl₃) δ 7.32−7.08 (m, 5H), 6.21 (s, 1H), 5.57 (s, 1H), 5.37−5.25 (m, 2H), 3.58−3.45 (m, 1H), 3.24 (dd, *J* = 14.5, 5.4 Hz, 1H), 3.05 (dd, *J* = 15.7, 11.7 Hz, 5H), 2.88 (s, 3H), 2.36−2.16 (m, 3H), 1.31 (s, 9H), 1.02 (s, 3H), 0.94 (s, 3H); ¹³C NMR (126 MHz, CDCl₃) δ 170.48, 169.37, 148.40, 141.17, 137.28, 130.83, 128.93, 128.46, 126.47, 121.17, 71.68, 57.23, 56.73, 51.12, 50.44, 48.77, 42.25, 37.16, 36.70, 34.13, 33.13,

33.01, 32.28, 31.58, 31.54, 30.26, 28.71, 20.62, 19.32, 16.74; MS (EI, m/z) = 532 (M$^+$); HRMS (EI): calcd for $C_{34}H_{48}N_2O_3$, 532.3665; found, 532.3668.

(3S,10R,13S)-N-((R)-1-(tert-Butylamino)-1-oxo-3-phenylpropan-2-yl)-3-hydroxy-N,10,13-trimethyl-2,3,4,7,8,9,10,11,12,13,14,15-do-decahydro-1H-cyclopenta[a]phenanthrene-17-carboxamide (18b). $[\alpha]_D^{20} = -191.739$ (c 0.230, CHCl$_3$); ^{1}H NMR (300 MHz, CDCl$_3$) δ 7.34−7.09 (m, 5H), 6.36 (s, 1H), 5.48 (s, 1H), 5.40−5.26 (m, 2H), 3.59−3.43 (m, 1H), 3.25 (dd, J = 15.1, 6.4 Hz, 1H), 3.01 (dd, J = 15.0, 10.1 Hz, 1H), 2.87 (s, 3H), 2.35−2.12 (m, 3H), 1.30 (s, 9H), 1.03 (s, 3H), 1.02 (s, 3H); ^{13}C NMR (126 MHz, CDCl$_3$) δ 171.10, 169.49, 148.07, 141.16, 137.42, 132.91, 128.79, 128.46, 126.46, 121.17, 71.67, 56.62, 56.44, 51.02, 50.52, 48.56, 42.26, 37.19, 36.74, 34.01, 32.87, 32.36, 31.59, 31.55, 30.13, 28.70, 20.61, 19.35, 16.58; MS (EI, m/z) = 532 (M$^+$); HRMS (EI): calcd for $C_{34}H_{48}N_2O_3$, 532.3665; found, 532.3661.

Crystallographic Data. Crystallographic data have been deposited in the Cambridge Crystallographic Data Centre (CCDC numbers CCDC 1421370, CCDC 1421371, and CCDC 1421406). Copies of the data can be obtained free of charge by application to Director, CCDC, 12 Union Road, Cambridge CB21EZ, UK (fax: +44 (0)1223 336033; e-mail: deposit@ccdc.cam.ac.uk).

Biology. *Cell Culture.* The BV-2 microglial cell line, HAPI rat microglial cell line, and HT-22 immortalized mouse hippocampal neuronal cell line were cultured in DMEM with 10% FBS and 1% penicillin/streptomycin at 37 °C with 5% CO$_2$. Primary microglia and primary astrocytes were cultured from the cerebral cortices of newborn (1 to 2 day old) mice from the Institute of Cancer Research (ICR) as described previously.[24] The purity of microglial cells and astrocytes (>95%) was determined by CD11b or GFAP immunostaining (data not shown). All animal experiments were conducted according to the guidelines of the National Institutes of Health and Soochow University's protocol on animal use and care.

Quantification of Nitrite, TNF-α, IL-6, and PGE-2. Microglial cells or astrocytes were seeded in 96-well plates at a density of 2×10^4 cells/well. The cells were pretreated with different concentration of compounds for 30 min before being stimulated with LPS (0.1 μg/mL) for 24 h. The cell culture medium was collected, and the concentration of nitrite was measured by Griess reagents. The levels of TNF-α, IL-6, and PGE-2 in the supernatants were determined by specific ELISA kits (R&D Systems).[24]

Quantitative Real-Time Polymerase Chain Reaction. BV-2 cells were seeded in 6-well plates at a density of 2×10^5 cells/well. The cells were pretreated with different concentrations of compounds for 30 min before being stimulated with LPS (0.1 μg/mL) for 6 h. Then, total RNA was isolated with TRIzol reagent (Takara, Dalian China). For the synthesis of cDNA, 1 μg of total RNA was reverse-transcribed using a reverse-transcription kit according to the manufacturer's instruction. RT-PCR was conducted using cDNA and SYBR Green qPCR master mix (Roche, USA). The specific primer sets used have been previously reported.[24] The relative expression of the target gene mRNA was calculated using the $2^{-\Delta\Delta C_T}$ method.[8]

Western Blot. BV-2 microglial cells were seeded in 6-well plates at a density of 2×10^5 cells/well. The cells were preincubated with compound **18b** for 30 min and then stimulated with LPS (0.1 μg/mL). After stimulation with LPS for 16 h, total protein was isolated with RIPA protein lysis buffer. Forty micrograms of the cell lysate was used for western blot analysis as described previously. The following primary and second antibodies were used for western blot analysis: antibodies against iNOS and COX-2 were purchased from Abcam (Cambridge, MA); antibodies against total and phospho-IκB and phospho-IKK as well as total and phospho-MAPKs were purchased from Cell Signaling Technology (Beverly, MA); antibodies against α-tubulin and horseradish peroxidase-conjugated secondary antibodies were purchased from Sigma-Aldrich (St. Louis, MO).

Luciferase Reporter Assay. The BV-2 cells that stably expressed the NF-κB or AP-1 lentiviral reporter construct (CignalTM Lenti Reporters, Qiagen) were established as previously described.[25] The established cell lines were preincubated with compound **18b** for 30 min. After stimulation with LPS (0.1 μg/mL) for 16 h, enzyme luminescent activity was measured using the luciferase assay kit (Promega) according to the manufacturer's instruction. The data are expressed as relative values of luciferase activity.

Microglial-Conditioned Medium/Neuron Coculture. The coculture of microglial-CM and neurons was performed as described previously.[26] In brief, BV-2 microglial cells were seeded in 6-well plates at a density of 2×10^5 cells/well. The BV-2 microglial cells were preincubated with compound **18b** for 30 min. After stimulation with LPS (0.1 μg/mL) for 24 h, the CM was harvested and added to the 24-well plate containing HT-22 neuroblastoma cells. After the incubation of HT-22 cells with the CM for 36 h, cell viability was assessed by MTT assay.

Experimental Ischemic Mouse Model. A total of 20 male ICR mice weighting 20−30 g (SLAC, Shanghai, China) at the beginning of each experiment received MCAO surgery. The mice were randomly divided into two groups that received either intraperitoneal injection of compound **18b** (40 mg/mL, n = 10) or injection of an equal volume of saline (n = 10) for 1 h before MCAO. The dose of compound **18b** was chosen based on a preliminary experiment showing its anti-inflammatory effect on an LPS-induced (stereotaxic injection) mouse neuroinflammation model (data not shown). Transient mouse focal cerebral ischemia was carried out as described as previously.[21] Briefly, mice were anesthetized with 1.5% isoflurane in 30% O$_2$ and 70% N$_2$O. The body temperature of the mice was sustained at 37 °C with a heating pad during all surgical procedures. The common carotid artery, bifurcation of the external carotid artery, and internal carotid artery were exposed before the insertion of a silicon-coated nylon monofilament (diameter 0.22 ± 0.02 mm). To confirm successful occlusion, cerebral blood flow in the middle carotid artery was monitored by a laser Doppler flowmeter. A reduction of 70% from the baseline was considered as a successful occlusion. For reperfusion, the filament was removed after 60 min of occlusion. After 24 h of reperfusion, the mice were sacrificed and perfused with saline (n = 4). The brains were quickly removed, coronally sliced into 2 mm thick sections, and then stained with 1% 2,3,5-triphenyltetrazolium chloride (TTC) in saline at 37 °C (water bath) for 10 min. After incubation with TTC, the sections were fixed with 10% formaldehyde in PB buffer for 24 h. The fixed sections were imaged using a scanner, and the total infarct volume and volume corrected for brain edema were calculated by image analysis software (SigmaScan Pro, Jandel, San Rafael, CA) as describe previously.[21] For the TTC staining, three mice died in both the compound **18b** and saline groups after MCAO; three mice were eliminated in both the compound **18b** and saline groups because their cerebral blood flow did not meet the requirement of standard of MCAO. For the RT-PCR analysis, two and three mice died after MCAO in the compound **18b** and saline groups, respectively; four and three mice were eliminated in the compound **18b** and saline groups, respectively. For compound administration, compound **18b** was dissolved in a 5% 2-hydroxypropyl-β-cyclodextrin/0.5% carboxymethylcellulose sodium solution. The animal experiments were approved by Institutional Review Board of Soochow University. The care and use of animals in the present study were performed in accordance with the guidelines of the National Institutes of Health.

Statistical Analysis. All data in the figures, tables, and text are expressed as the mean ± SD. One-way ANOVA followed by the Student−Newman−Keuls *post hoc* analysis was used for the multiple comparisons. Values of $P < 0.05$ were considered significant.

■ ASSOCIATED CONTENT

Ⓢ Supporting Information

The Supporting Information is available free of charge on the ACS Publications website at DOI: 10.1021/acschemneuro.5b00256.

^{1}H and ^{13}C NMR of target compounds (PDF)

■ AUTHOR INFORMATION

Corresponding Authors

*(H.C.) Phone: +86 2120685035. E-mail: chenhl@shanghaitech.edu.cn.

*(L.T.Z.) Phone: +86 2120685035. E-mail: zhenglongtai@suda.edu.cn.

*(B.J.) Phone: +86 2120685035. E-mail: jiangbiao@shanghaitech.edu.cn.

Author Contributions

§H.C., C.H., and J.W. contributed equally to this work.

■ ABBREVIATIONS

NO, nitric oxide; TNF-α, tumor necrosis factor-α; IL-1β, interleukin-1β; IL-6, interleukin-6; iNOS, inducible nitric oxide synthase; LPS, lipopolysaccharide; U-4CC, Ugi four-component condensation

■ REFERENCES

(1) Qin, L., Wu, X., Block, M. L., Liu, Y., Breese, G. R., Hong, J. S., Knapp, D. J., and Crews, F. T. (2007) Systemic LPS causes chronic neuroinflammation and progressive neurodegeneration. *Glia 55*, 453−462.

(2) Baldwin, K. T., Carbajal, K. S., Segal, B. M., and Giger, R. J. (2015) Neuroinflammation triggered by beta-glucan/dectin-1 signaling enables CNS axon regeneration. *Proc. Natl. Acad. Sci. U. S. A. 112*, 2581−2586.

(3) Ransohoff, R. M., Schafer, D., Vincent, A., Blachere, N. E., and Bar-Or, A. (2015) Neuroinflammation: Ways in Which the Immune System Affects the Brain. *Neurotherapeutics 12*, 896−909.

(4) Saijo, K., and Glass, C. K. (2011) Microglial cell origin and phenotypes in health and disease. *Nat. Rev. Immunol. 11*, 775−787.

(5) Klegeris, A., McGeer, E. G., and McGeer, P. L. (2007) Therapeutic approaches to inflammation in neurodegenerative disease. *Curr. Opin. Neurol. 20*, 351−357.

(6) Giatti, S., Boraso, M., Melcangi, R. C., and Viviani, B. (2012) Neuroactive steroids, their metabolites, and neuroinflammation. *J. Mol. Endocrinol. 49*, R125−R134.

(7) Wang, M. J., Huang, H. M., Chen, H. L., Kuo, J. S., and Jeng, K. C. G. (2001) Dehydroepiandrosterone inhibits lipopolysaccharide-induced nitric oxide production in BV-2 microglia. *J. Neurochem. 77*, 830−838.

(8) Yang, Y. X., Zheng, L. T., Shi, J. J., Gao, B., Chen, Y. K., Yang, H. C., Chen, H. L., Li, Y. C., and Zhen, X. C. (2014) Synthesis of 5alpha-cholestan-6-one derivatives and their inhibitory activities of NO production in activated microglia: discovery of a novel neuroinflammation inhibitor. *Bioorg. Med. Chem. Lett. 24*, 1222−1227.

(9) Wu, J., Du, J. J., Gu, R. N., Zhang, L., Zhen, X. C., Li, Y. C., Chen, H. L., Jiang, B. A., and Zheng, L. T. (2015) Inhibition of Neuroinflammation by Synthetic Androstene Derivatives Incorporating Amino Acid Methyl Esters on Activated BV-2 Microglia. *ChemMedChem 10*, 610−616.

(10) Domling, A., and Ugi, I. (2000) Multicomponent reactions with isocyanides. *Angew. Chem., Int. Ed. 39*, 3168−3210.

(11) Domling, A., Wang, W., and Wang, K. (2012) Chemistry and biology of multicomponent reactions. *Chem. Rev. 112*, 3083−3135.

(12) Ramozzi, R., Cheron, N., El Kaim, L., Grimaud, L., and Fleurat-Lessard, P. (2014) Predicting new Ugi-smiles couplings: a combined experimental and theoretical study. *Chem. - Eur. J. 20*, 9094−9099.

(13) Varadi, A., Palmer, T. C., Haselton, N., Afonin, D., Subrath, J. J., Le Rouzic, V., Hunkele, A., Pasternak, G. W., Marrone, G. F., Borics, A., and Majumdar, S. (2015) Synthesis of Carfentanil Amide Opioids Using the Ugi Multicomponent Reaction. *ACS Chem. Neurosci. 6*, 1570−1577.

(14) Zhu, N., Ling, Y., Lei, X., Handratta, V., and Brodie, A. M. (2003) Novel P450(17alpha) inhibitors: 17-(2′-oxazolyl)- and 17-(2′-thiazolyl)-androstene derivatives. *Steroids 68*, 603−611.

(15) Garcia-Bonilla, L., Moore, J. M., Racchumi, G., Zhou, P., Butler, J. M., Iadecola, C., and Anrather, J. (2014) Inducible nitric oxide synthase in neutrophils and endothelium contributes to ischemic brain injury in mice. *J. Immunol. 193*, 2531−2537.

(16) Iadecola, C. (1997) Bright and dark sides of nitric oxide in ischemic brain injury. *Trends Neurosci. 20*, 132−139.

(17) Nagafuji, T., Sugiyama, M., Matsui, T., Muto, A., and Naito, S. (1995) Nitric oxide synthase in cerebral ischemia. Possible contribution of nitric oxide synthase activation in brain microvessels to cerebral ischemic injury. *Mol. Chem. Neuropathol. 26*, 107−157.

(18) Liu, B., and Hong, J. S. (2003) Role of microglia in inflammation-mediated neurodegenerative diseases: mechanisms and strategies for therapeutic intervention. *J. Pharmacol. Exp. Ther. 304*, 1−7.

(19) Ghosh, S., May, M. J., and Kopp, E. B. (1998) NF-kappa B and Rel proteins: evolutionarily conserved mediators of immune responses. *Annu. Rev. Immunol. 16*, 225−260.

(20) Kaminska, B. (2005) MAPK signalling pathways as molecular targets for anti-inflammatory therapy - from molecular mechanisms to therapeutic benefits. *Biochim. Biophys. Acta, Proteins Proteomics 1754*, 253−262.

(21) Jin, Q., Cheng, J., Liu, Y., Wu, J., Wang, X. Y., Wei, S. W., Zhou, X. M., Qin, Z. H., Jia, J., and Zhen, X. C. (2014) Improvement of functional recovery by chronic metformin treatment is associated with enhanced alternative activation of microglia/macrophages and increased angiogenesis and neurogenesis following experimental stroke. *Brain, Behav., Immun. 40*, 131−142.

(22) Ginsberg, M. D. (2003) Adventures in the pathophysiology of brain ischemia: Penumbra, gene expression, neuroprotection - The 2002 Thomas Willis Lecture. *Stroke 34*, 214−223.

(23) Shin, J. A., Lee, H., Lim, Y. K., Koh, Y., Choi, J. H., and Park, E. M. (2010) Therapeutic effects of resveratrol during acute periods following experimental ischemic stroke. *J. Neuroimmunol. 227*, 93−100.

(24) Xu, Z. X., Wu, J., Zheng, J. Y., Ma, H. K., Zhang, H. J., Zhen, X. C., Zheng, L. T., and Zhang, X. H. (2015) Design, synthesis and evaluation of a series of non-steroidal anti-inflammatory drug conjugates as novel neuroinflammatory inhibitors. *Int. Immunopharmacol. 25*, 528−537.

(25) Zhou, X., Gan, P., Hao, L. L., Tao, L., Jia, J., Gao, B., Liu, J. Y., Zheng, L. T., and Zhen, X. C. (2014) Antiinflammatory Effects of Orientin-2 ″-O-Galactopyranoside on Lipopolysaccharide-Stimulated Microglia. *Biol. Pharm. Bull. 37*, 1282−1294.

(26) Tao, L., Zhang, F. L., Hao, L. L., Wu, J., Jia, J., Liu, J. Y., Zheng, L. T., and Zhen, X. C. (2014) 1-O-Tigloyl-1-O-deacetyl-nimbolinin B Inhibits LPS-Stimulated Inflammatory Responses by Suppressing NF-kappa B and JNK Activation in Microglia Cells. *J. Pharmacol. Sci. 125*, 364−374.